Imaging microwave electric fields using a near-field scanning microwave microscope

S. K. Dutta, C. P. Vlahacos, D. E. Steinhauer, Ashfaq S. Thanawalla, B. J. Feenstra, F. C. Wellstood, and Steven M. Anlage
Center for Superconductivity Research, Department of Physics, University of Maryland, College Park, Maryland 20742-4111

Harvey S. Newman
Naval Research Laboratory, Washington, DC 20375

(Received 5 August 1998; accepted for publication 5 November 1998)

By scanning a fine open-ended coaxial probe above an operating microwave device, we image local electric fields generated by the device at microwave frequencies. The probe is sensitive to the electric flux normal to the face of its center conductor, allowing different components of the field to be imaged by orienting the probe appropriately. Using a simple model of the microscope, we are able to interpret the system's output and determine the magnitude of the electric field at the probe tip. We show images of electric field components above a copper microstrip transmission line driven at 8 GHz, with a spatial resolution of approximately 200 μm. © *1999 American Institute of Physics.* [S0003-6951(99)05201-8]

Simulating the electromagnetic behavior of passive microwave devices provides an attractive route toward developing new and improved devices. Ultimately, the information obtained from such simulations includes the scattering parameters and the direction and magnitude of the electric fields near the device. To check the reliability of these results, one can go beyond standard *S*-parameter measurements, and use imaging techniques to determine the electromagnetic fields experimentally. Methods for imaging local electric fields include using modulated scatterer probes,[1] coaxial cable probes,[2–5] electrooptic sampling,[6,7] extensions of atomic force microscopy,[8] and scanning superconducting quantum interference device (SQUID) microscopy.[9] Most of these techniques require expensive components and complicated configurations. In this letter, we describe the use of a relatively simple technique, employing an open-ended coaxial probe to image the vector components of the local electric field generated by operating microwave circuits. In addition, we discuss how to interpret the images in terms of electric fields present at the face of the probe.

Our experimental configuration is shown schematically in Fig. 1.[4] We use a coaxial cable probe with a center conductor diameter $d_c = 200\,\mu$m and an outer diameter $d_0 = 860\,\mu$m. During a scan, the probe is held at a constant height h above the sample, typically between 10 μm and several millimeters. Radio frequency (rf) electric fields from the sample induce a high-frequency potential difference between the center and grounded outer conductors of the probe. The probe is connected to the input port of a directional coupler, which has a length of coaxial cable attached to its output port, thereby creating a resonant circuit. The coupled port of the directional coupler is connected to a matched diode detector, which produces a voltage output proportional to the incident rf power. The diode voltage is low-pass filtered, amplified, and recorded by a computer. The computer also controls a two-axis translation stage, which raster scans the sample underneath the probe.

The relationship between the diode voltage output and the electric field at the probe face can be found by analyzing a circuit model for the system. The main idea is that the charge Q induced on the exposed face of the probe's center conductor is proportional to the integral of the normal component of the electric field E_n over this face. We note that this naturally limits the spatial resolution of the technique to no better than the diameter of the center conductor. The induced current at the probe face is then $I = \dot{Q} = i\omega\epsilon_0 E_n A$, where A is the area of the center conductor face and ω is the angular frequency of the microwave field.

In order to relate I to the voltage in the probe-coupler-cable assembly, we need to know the impedance Z_m that this microscope assembly presents to an input signal. Using standard transmission line theory,[10] we find

$$Z_m = Z_0\left[\frac{(Z_c+Z_0)+(1-\delta)^2(Z_c-Z_0)}{(Z_c+Z_0)-(1-\delta)^2(Z_c-Z_0)}\right], \tag{1}$$

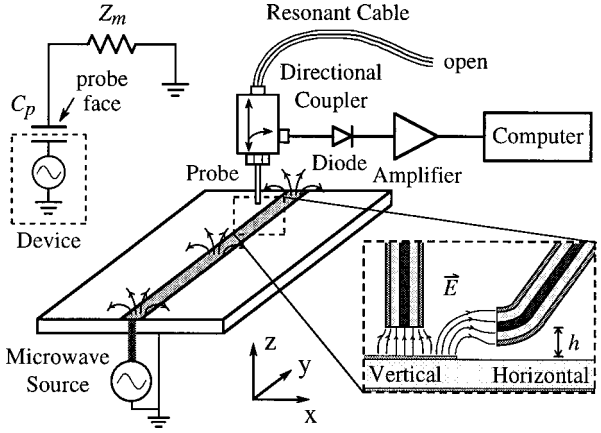

FIG. 1. Schematic showing the main components of the microwave microscope. An open-ended coaxial probe is brought near an operating device, so that stray electric fields induce a microwave signal in the probe. The inset in the lower right shows probe orientations used to measure different field components, at a common probe/sample separation h. The inset in the upper left shows the interaction of the device with the microscope.

where $Z_0 = 50\,\Omega$ is the characteristic impedance of the transmission line, Z_c is the input impedance of the resonant cable,[10] and δ is the fraction of the input signal voltage that the directional coupler taps off to its coupled port. For the parameters of the resonant section used (2 m long, open-ended cable with an attenuation of 1.1 dB/m, driven at resonance near 8 GHz), $Z_c \approx 200\,\Omega$. As a result, for our -10 dB ($\delta \approx 0.3$) directional coupler, one finds $Z_m \approx 90\,\Omega$.

By equating the current in the cable assembly to the current generated by the field, we can solve for the root mean square (rms) magnitude of the field at the probe in terms of the measured diode voltage

$$|E_n| = \frac{2}{\omega \epsilon_0 A \delta |Z_m + Z_0|} D(V_{\mathrm{dc}}), \tag{2}$$

where D is the high-frequency rms voltage at the diode input corresponding to the measured diode output voltage V_{dc}.

The use of a coaxial probe geometry has several consequences for the correct interpretation of Eq. (2). First, the expression is valid provided we take E_n to represent the field at the probe face when the probe is present. In general, this field may differ significantly from the field E_n^0 in the absence of the probe. The nature of the perturbation due to the probe is discussed in more detail below. Second, the derivation of Eq. (2) assumes that the coupling between the coaxial probe and the device primarily occurs via the exposed face of the center conductor, i.e., only the field normal to this face is detected. Because the outer conductor shields the transverse components of the electric field, this assumption is justified. This shielding means we can image individual components of the field by orienting the face of the probe in the appropriate direction. The inset in the lower right of Fig. 1 shows two such orientations, denoted ''vertical'' (probe face in the *xy* plane) and ''horizontal'' (probe face in the *yz* plane).

To investigate the capabilities of the microscope, we imaged a simple copper microstrip transmission line (see Fig. 1). The microstrip consists of a ground plane and a 2-mm-wide and 45-mm-long strip which are each 30 μm thick and separated by a 1.5-mm-thick dielectric ($\epsilon_r \approx 3.55$). We connected a microwave source directly to one end of the strip while the opposite end was left open, so that standing waves form with a voltage antinode at the open end.

Figure 2(a) shows an image of a single antinode in the middle of the strip, where the dashed lines indicate the edges of the strip.[11] Here, the probe was in the vertical orientation with $h = 25\,\mu$m and the source frequency was 8.05 GHz. The wavelength of the standing wave pattern was observed to decrease with increasing source frequency, as expected.[5] We note that the field peaks strongly just within the edges of the strip and that there are weak lobes away from the strip.

Orienting the probe horizontally with the probe face pointing in the negative $\hat{x}$ direction (as in the lower right inset of Fig. 1) with $h = 455\,\mu$m results in a rather different image [see Fig. 2(b)]. In contrast to Fig. 2(a), note that the peak at $X > 0$ in Fig. 2(b) is located well outside the strip. Furthermore, notice that the peak at $X < 0$ is much weaker. Compared to the vertical configuration, in the horizontal orientation, the outer conductor more strongly perturbs the field when situated over the strip, thereby decreasing the signal and causing an asymmetry in the final image. In order to accurately image the peak at $X < 0$, the probe must be rotated such that its face points in the positive $\hat{x}$ direction, i.e., the mirror image of the orientation in the inset to Fig. 1.

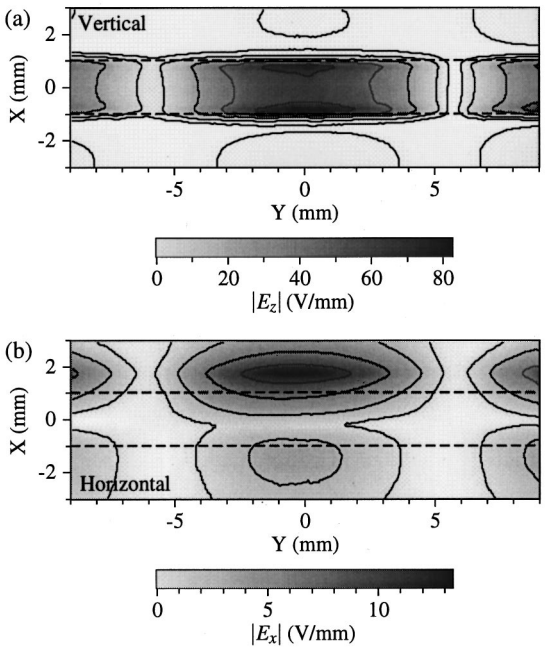

FIG. 2. Images of two components of electric field taken above a 2-mm-wide copper microstrip driven at 8.05 GHz. The dashed lines show the boundaries of the strip. (a) Image with vertical probe ($h = 25\,\mu$m); contour lines at 70, 50, 30, 10, and 3 V/mm. (b) Image with horizontal probe ($h = 455\,\mu$m); contour lines at 11, 7.5, 4, and 1.5 V/mm.

The most important issue, however, is the remarkable difference in the signal measured for different probe orientations. Figures 3(a) and 3(b) show that this difference is also evident when the sample is scanned in the *xz* plane. For example, the field decreases more rapidly with increasing height for the vertical probe than the horizontal probe (note that for the horizontal probe orientation, the smallest probe/sample separation is limited by the outer conductor radius).

The fact that the images depend strongly on probe orientation is consistent with the probe being sensitive to individual components of electric field. To compare the data with the expected field profile at a standing wave antinode [i.e., a slice in the *xz* plane, such as in Figs. 3(a) and 3(b)], we model the microstrip as a conductor held at a constant potential above a grounded plane. We then find the electric field by numerically solving Poisson's equation in the inhomogeneous medium surrounding the conductors and averaging the result over the area of the probe's center conductor.

Naturally, we expect only qualitative agreement between the static model and the data. First of all, the model is not a full-wave solution at microwave frequencies for inhomogeneous microstrip.[12] In addition, it neglects the presence of the microscope. For instance, the grounded outer conductor of the probe causes a local redistribution and screening of electric field (more pronounced when using a horizontal probe). Also, the current delivered by the sample to the microscope will depend on its capacitive coupling C_p to the probe and on the value of Z_m. In the unperturbed case, the potential on a small segment of the strip sees a path to ground via the vacuum. However, with the probe present, the voltage is dropped across the probe/sample impedance Z_p

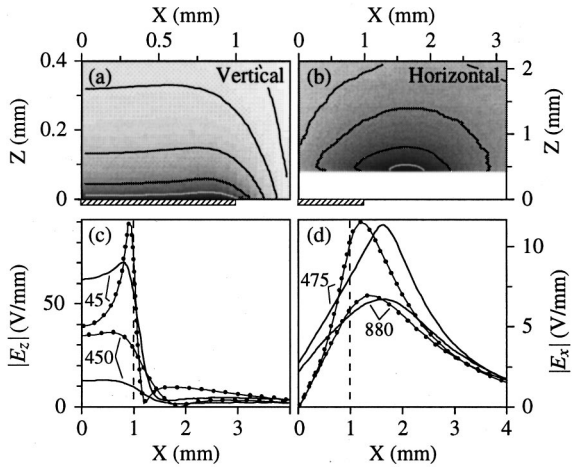

FIG. 3. Electric field in the *xz* plane above the microstrip (at $Y=0$ in Fig. 2) with the probe (a) vertical (contour lines at 80, 55, 30, 15, and 8 V/mm) and (b) horizontal (contour lines at 12, 9, 6, and 4 V/mm). The strip is shown as a hatched rectangle on the *x* axes. Solid lines in (c) and (d) show line cuts (at $Y=0$) of experimental data at two probe heights, as labeled in μm. The dotted lines show the corresponding numerical field simulation, neglecting probe perturbation. The vertical simulation data are multiplied by 65 and the horizontal by 25. The dashed vertical lines show the edge of the strip.

$=1/i\omega C_p$ and Z_m (see inset in upper left of Fig. 1). Clearly, the value of these two impedances will have a significant effect on the measured electric field.

Figure 3(c) shows constant-height line scans above the strip for the experimental data (solid) and model calculations (dotted) for the vertical (E_z) probe orientation. Figure 3(d) shows the corresponding data for the horizontal (E_x) probe orientation. In order to make the magnitude of the fields comparable, the simulation values have been scaled up by a factor of 65 for the vertical and 25 for the horizontal orientation. We note that despite the simplifying assumptions made in our model, the experimental results reproduce three key features in the simulations which are consistent with the imaging of separate field components: (i) E_z is large at the center of the strip, while E_x is nearly zero; (ii) E_z peaks just inside the strip edge, while E_x peaks outside; and (iii) $|E_z|$ has a minimum just to the side of the strip, while E_x dies off slowly and monotonically to zero, away from the strip.

Although the experimental and model curves are qualitatively similar, there are large quantitative differences. This is largely due to the fact that the perturbation caused by the probe has not been taken into account in the static electric field model. To make a quantitative comparison between experiment and theory, it is essential to calculate the field with the probe present. By knowing the values of Z_p and Z_m, and the voltage at some point on the strip, we can find the voltage drop across Z_p and directly determine the value of the perturbed electric field at that location. Treating the probe/sample capacitance C_p as a parallel plate capacitor yields $C_p \approx 6$ fF ($|Z_p| \approx 3.2\,\mathrm{k}\Omega$ at 8 GHz) for a vertical probe at $h=45\ \mu$m.[13] From independent measurements, the rms voltage at the center of an antinode [e.g., $X=0$, $Y=0$ in Fig. 2(a)] was found to be 1.25 V. With these values, we estimate $|E_z| \approx 27$ V/mm. In comparison, the experimental value is 62 V/mm and the simple model yields 0.6 V/mm. Thus, the measured electric field is enhanced in a manner consistent with our expectations.

The data presented in Figs. 2 and 3 have an uncertainty of approximately 1% for the peak values and 4% for the regions far from the strip. However, uncertainty in probe height ($\sim 5\ \mu$m) may give rise to a large effective decrease in the precision, especially if the field is strongly dependent on height. From Eq. (2), one sees that the diode voltage scales roughly as the area of the center conductor for a given electric field. Therefore at 8 GHz, for the $d_c = 200\ \mu$m probe used here, the microscope works well for field strengths greater than 0.5 V/mm, while a larger probe ($d_c = 510\ \mu$m) would operate precisely above 0.1 V/mm. The electric field sensitivity is mainly limited by the sensitivity of the electronics and the 20 ms averaging time. It could be significantly enhanced by using a low-noise amplifier or phase-sensitive detection of an amplitude-modulated signal. However, the present sensitivity is already sufficient for the application of this imaging technique to, for instance, superconducting filters.[14]

In conclusion, using a near-field scanning microwave microscope, we have demonstrated the imaging of individual components of electric field above a microstrip line. The microscope is composed of simple components and has a wide range of operation (about 80 MHz to 50 GHz). Although the coaxial probe perturbs the fields it is measuring, the mechanism for this perturbation is understood. In principle, it should be possible to correct for this effect. Finally, we note that scanning can be done fairly quickly; Fig. 2 was sampled at a rate of 50 Hz with a spatial resolution of 50 μm, yielding an image in about 15 min.

The authors wish to acknowledge useful discussions with D. W. van der Weide. This work has been supported by NSF Grant No. ECS-9632811, NSF-MRSEC Grant No. DMR-9632521, and by the Maryland Center for Superconductivity Research.

[1] T. P. Budka, S. D. Waclawik, and G. M. Rebeiz, IEEE Trans. Microwave Theory Tech. **44**, 2174 (1996), and references therein.
[2] Y. Gao and I. Wolff, IEEE MTT-S Int. Microwave Symp. Dig. **3**, 1537 (1996).
[3] C. Gao, T. Wei, F. Duewer, Y. Lu, and X.-D. Xiang, Appl. Phys. Lett. **71**, 1872 (1997).
[4] C. P. Vlahacos, R. C. Black, S. M. Anlage, A. Amar, and F. C. Wellstood, Appl. Phys. Lett. **69**, 3272 (1996).
[5] S. M. Anlage, C. P. Vlahacos, S. Dutta, and F. C. Wellstood, IEEE Trans. Appl. Supercond. **7**, 3686 (1997).
[6] A. S. Hou, F. Ho, and D. M. Bloom, Electron. Lett. **28**, 2302 (1992).
[7] K. J. Weingarten, M. J. W. Rodwell, and D. M. Bloom, IEEE J. Quantum Electron. **24**, 198 (1988).
[8] D. W. van der Weide and P. Neuzil, J. Vac. Sci. Technol. B **14**, 4144 (1996).
[9] S. Chatraphorn, E. F. Fleet, R. C. Black, and F. C. Wellstood, Appl. Phys. Lett. **73**, 984 (1998).
[10] S. Ramo, J. R. Whinnery, and T. Van Duzer, *Fields and Communication Electronics*, 3rd ed. (Wiley, New York, 1994).
[11] A small constant offset was subtracted from all plots, on the basis that the field should vanish far from the strip.
[12] R. K. Hoffmann, *Handbook of Microwave Integrated Circuits* (Artech House, Norwood, MA, 1987), p. 135.
[13] For $Z_p = 3.2\ \mathrm{k}\Omega$ and $Z_m = 90\ \Omega$, even substantial changes in Z_c and δ will not significantly affect the value of the measured electric field.
[14] A. S. Thanawalla, S. K. Dutta, C. P. Vlahacos, D. E. Steinhauer, B. J. Feenstra, Steven M. Anlage, F. C. Wellstood, and R. B. Hammond, Appl. Phys. Lett. **73**, 2491 (1998).